ACS APPLIED MATERIALS & INTERFACES

Research Article

www.acsami.org

CAF@ZIF-8: One-Step Encapsulation of Caffeine in MOF

Nuria Liédana, Alejandro Galve, César Rubio, Carlos Téllez, and Joaquín Coronas*

Chemical and Environmental Engineering Department and Instituto de Nanociencia de Aragón (INA), Universidad de Zaragoza, 50018 Zaragoza, Spain

Supporting Information

ABSTRACT: Two strategies for encapsulating caffeine in ZIF-8 were carried out in this work: (1) one-step, in situ encapsulation where caffeine is added to a ZIF-8 synthesis solution and the MOF structure is formed around the entrapped molecule; and (2) ex situ encapsulation whereby caffeine is put into contact with previously synthesized or purchased ZIF-8. The products obtained were analyzed with XRD, TGA, Vis-UV, GC-MS, FTIR, ^{13}C NMR, and N 1s XPS to compare both encapsulation methods. Chemical and structural evidence indicated that the preferential adsorption site of caffeine molecules inside the ZIF-8 structure is near the methyl and CH groups of 2-methylimidazole ligand. These two groups interact with caffeine by van der Waals forces with methyl groups and via CH···O hydrogen bonds with C═O groups, respectively. In addition, the one-step encapsulation of caffeine in ZIF-8 produced high guest loading (ca. 28 wt % in only 2 h at 25 °C) and controlled release (during 27 days).

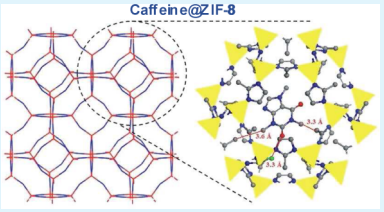

KEYWORDS: *metal organic framework, ZIF-8, encapsulation, caffeine, drug delivery*

INTRODUCTION

Metal−organic frameworks (MOFs) are hybrid materials composed of metal ions joined to organic linkers which act like a bridge between metal centers.[1] The final network is highly porous with large specific surface area,[2] tunable pore size,[3] shape,[4] and functionality.[5] They are very attractive materials with potential applications in the fields of adsorption,[3] medicine,[6] membranes,[7] catalysis,[8] and separation and storage of gases and vapors.[9]

Thanks to their large specific surface area, MOFs have contributed to developments in the biomedical field concerning drug delivery[10] and imaging techniques.[11] In fact, these applications relate to encapsulation, a tool useful also for producing high-performance catalysts by direct encapsulation (in one-pot synthesis) of polyoxometalates (POMs) in MIL-101(Cr).[12] In addition, bio-MOF-1, an anionic Zn-adeninate MOF, encapsulates by ion exchange lanthanide cations giving rise to materials with a potential application as high surface area sensors for small molecules.[13] POMs of the Keggin structure have been encapsulated by simple one-pot hydrothermal synthesis in HKUST-1[14] and NH_2-MIL-101(Al)[15] demonstrating advantages such as dispersion at the molecular level[14a] and a templating effect.[14a,15]

Caffeine is an amphiphilic drug with significant lipolytic activity, becoming a very useful agent mainly in the cosmetic industry. Caffeine molecules have often been used as a model active ingredient, so many formulations of caffeine contained within several different matrices have been studied. These include cyclodextrines,[16] liposomes and niosomes,[17] poly-(epsilon-caprolactone) polymer,[18] PLGA-mPEG copolymers,[19] protein concentrate hydrogels,[20] and silica[21] as the most notable hosts. In this work, we present a versatile strategy for the one-pot encapsulation of caffeine in zeolitic imidazolate ZIF-8.[22] In particular, we show that a larger amount of caffeine can be encapsulated with this strategy when compared to encapsulation in two steps (MIL-88B_2OH,[23] and MIL-53 and MIL-100[24]), and that a slower release is achieved due to the strong interaction established between caffeine and ZIF-8. Furthermore, regarding hydrothermal stability, ZIF-8 is unique when compared to other MOFs bridged by carboxylates. It has been reported that this MOF was not significantly damaged under steaming at 300 °C,[25] which could be of interest in applications where high temperature processing is an issue, for instance, in the encapsulation of additives for polyamide fiber modification, a process in which the authors have some previous experience and in which the polymer has to be spun at about 260 °C.[26] In consequence, the encapsulation of caffeine, a model drug, in ZIF-8 would not only be a single mode of controlled release but also a way of providing thermal protection for a high temperature process. In this context, one-pot, in situ encapsulation reduces to one step the two traditional steps for encapsulation: synthesis and activation of the porous material and the final encapsulation of the additive. A rapid and efficient encapsulation methodology is demonstrated.

EXPERIMENTAL SECTION

Synthesis and Encapsulation Procedure. ZIF-8 containing caffeine was synthesized with reagents to form ZIF-8: 2-methylimidazole (99% purity, Sigma-Aldrich), $Zn(NO_3)_2{\cdot}6H_2O$ (98% grade, Sigma-Aldrich), and caffeine (1,3,7-trimethylxanthine, ReagentPlus, Sigma-Aldrich). For comparison purposes, ZIF-8, Basolite-Z1200, was purchased from Sigma-Aldrich. Methanol (Multisolvent HPLC grade, Scharlau) and deionized water were used as solvents.

Received: July 20, 2012
Accepted: July 26, 2012
Published: July 26, 2012

 © 2012 American Chemical Society dx.doi.org/10.1021/am301365h | ACS Appl. Mater. Interfaces 2012, 4, 5016−5021

To perform a one-step encapsulation of caffeine inside ZIF-8 pores (CAF@ZIF-8_IN), we prepared two solutions. The first solution contained 2-methylimidazole (3.09 g) in methanol (20 mL), whereas the second contained $Zn(NO_3)_2{\cdot}6H_2O$ (0.95 g), caffeine (0.6 g), methanol (20 mL), and water (10 mL). Methanol was used to increase the caffeine solubility in the final dispersion. When the reagents were dissolved, the solution containing $Zn(NO_3)_2{\cdot}6H_2O$ and caffeine was added to that with the linker. After 10 min a white suspension began to form, which was maintained at 25 °C under stirring for a total synthesis time of 2 h. It was subsequently centrifuged for 20 min, washed with methanol (5 mL) to remove any 2-methylimidazole excess and centrifuged again for 10 min. The total molar composition was $Zn(NO_3)_2{\cdot}6H_2O$:2-methylimidazole:methanol:H_2O:caffeine = 0.32:3.84:100:56.7:0.31.

To encapsulate caffeine with previously prepared materials (CAF@ZIF-8_EX), we used both commercial (Basolite Z1200) and the one obtained here (using the latter solution for CAF@ZIF-8_IN but without caffeine). The latter material does not require activation (see TGA in Figure S1 in the Supporting Information for ZIF-8). ZIF-8 material (2 g) was suspended in 100 mL of caffeine aqueous solution (40 g/L) and maintained under stirring at 80 °C for 8 h (commercial) and 1.5, 3, 5, and 7 days (the one made here). Once filtered and recovered, the CAF@ZIF-8_EX was dried at room temperature.

Characterization. The materials obtained and commercial ZIF-8 were analyzed by X-ray diffraction (XRD) using a D-Max Rigaku X-ray diffractometer with a copper anode and a graphite monochromator to select CuKα radiation (λ = 1.5418 Å).

The scanning electron microscopy images were taken with a Hitachi S2300 model at 10 kV. The powder samples were prepared over magnetic strip by coating with gold under vacuum conditions.

Thermogravimetric analyses were performed using Mettler Toledo TGA/SDTA 851e equipment. Samples placed in 70 μL alumina pans were heated in N_2 flow up to 750 °C with a heating rate of 10 °C/min.

Delivery measurements were carried out at room temperature with a V-670 Jasco UV−vis spectrophotometer. The measurements were taken at 272.5 nm, being the maximum absorption wavelength for the caffeine molecule with no overlapping with 2-methylimidazole absorbance (maximum at 203.5 nm, Figure S2). Suspensions of 50 mg of CAF@ZIF-8 materials in 500 mL of water were prepared and the concentration of caffeine in each 3 mL aliquot was determined using a calibration curve. Several caffeine-water solutions in the 0−30 mg/L concentration were prepared to obtain the calibration curve. The drug delivery results are the average of three different solid samples prepared and analyzed in the same way. All the release experiments were performed without stirring.

The GC/MS analysis was carried out with an Agilent 6850 gas chromatograph with a 5975C VL MSD mass spectrometric detector. Caffeine was separated by means of a HP-5MS capillary column, 30 m × 0.25 mm I.D. and 0.25 μm phase thickness. The He carrier gas was set at a constant flow-rate of 1 mL(STP)/min, and 1 μL sample solution was injected with a 1:50 split ratio. Injector and detector temperatures of the GC/MS were set at 250 and 280 °C, respectively. The GC oven was maintained at 120 °C for 2 min, ramped at 40 °C/min to 240 °C and held at this temperature for 2 min. The mass spectrometer was operated in the electron impact mode (EI, 70 eV) and m/z 194 ion was selected for monitoring. Caffeine was identified by direct comparison with caffeine standard on the basis of the retention time and mass spectral ion ratios. Finally, 1 mL of the solution to be analyzed was 25 times diluted in ethanol.

The Fourier transformed infrared spectroscopy (FTIR) absorption spectra were acquired at room temperature with an Iraffinity Shimadzu spectrophotometer. Spectra of the samples corresponded to 30 scans at a resolution of 4 cm^{-1}, using the KBr pellet technique.

X-ray photoelectron analysis (XPS) was performed with an Axis Ultra DLD (Kratos Tech.). The samples were mounted on a sample rod placed in the pretreatment chamber of the spectrometer and then evacuated at room temperature. The spectra were excited by the monochromatized Al Kα source (1486.6 eV) at 15 kV and 10 mA. A pass energy of 20 eV was used for the individual peak regions. Analyses of the peaks were performed using a weighted sum of Lorentzian and Gaussian components curves after background subtraction. The binding energies were referenced to the internal standard C 1s (284.5 eV).

The ^{13}C CP MAS NMR spectra were recorded on a Bruker AV-400-WB spectrometer operating at 75.45 MHz for ^{13}C with magic angle spinning (MAS) at 12 kHz. Solid samples were analyzed in a 4 mm zirconia rotor. Chemical shifts (δ) of ^{13}C nuclei were externally referred to 3-trimethylsilyl-1-propanesulfonic acid sodium salt (DDS) at δ = 0.0 ppm and the C═O group of glycine at δ = 176.1 ppm. A pulse width of 4 μs, a contact time of 2.5 ms and a recycle delay of 5 s were applied. Typically, 13 000 scans were collected.

Elemental analysis was carried out using a Flash EA 1112 Elemental Analyzer. Contents of C, H and N and O were determined by combustion and pyrolysis, respectively, of the sample and quantification of the gases produced. Before the analysis, the samples were treated at 230 °C for 30 min. The detection range was from 0.05 to 99.95%.

Structure Refinement. The structure of ZIF-8 with caffeine inside the pores was determined from the X-ray diffraction patterns using as a basic computational platform the Accelrys Materials Studio 4.3 software supplied by Accelrys. A combination of Rietveld[27] and Pawley[28] refinement methods was used for the optimum determination of the structures. Initially, Pawley refinement was performed until no improvement for weighted profile factor (R_{wp}) was observed. The order for parameter refinement was the following: first, baseline; second, parameters related to peak shape with the Pseudo-Voigt for peak profile and Berar-Baldinozzi for asymmetry models. Then the lattice parameters were refined, and finally all the parameters were refined together.

For Rietveld refinement, all the occupancies were first refined, followed by peak shape parameters and lattice parameters. Finally, all the parameters were refined at the same time. The optimum structure was selected based on the minimum achieved Rwp. Caffeine was added to the model inside the pores, and its position was refined together with the peak profile and asymmetry parameters.

RESULTS AND DISCUSSION

The in situ encapsulation of caffeine in ZIF-8 (CAF@ZIF-8_IN, i.e. the synthesis of ZIF-8 in the presence of the drug) took place for 2 h at 25 °C, leading to a caffeine load of 28.1 ± 2.6% (average of three different samples) as determined by TGA (Figure 1). The caffeine weight loss was considered in the

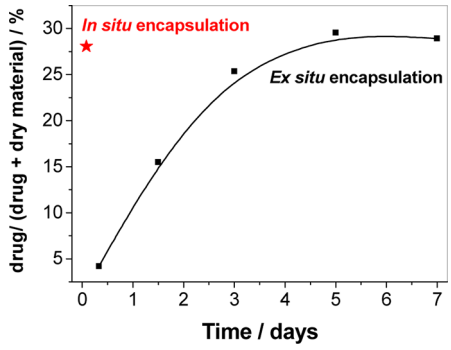

Figure 1. In situ and ex situ encapsulation of caffeine in ZIF-8 as determined by TGA.

325−525 °C range (see Figure S1 in the Supporting Information). Below 325 °C, free caffeine was responsible for the weight loss; above 525 °C the decomposition of ZIF-8 took place. To encapsulate appreciable amounts of caffeine by the ex situ process (CAF@ZIF-8_EX), we must prolong the contact at 80 °C for at least 8 h (4.2 ± 1.4%, Figure 1), and for about 3 days to achieve a similar result (Figure 1) as that given by the in situ procedure. Commercial ZIF-8 (BET area=1305 ± 17 m^2

g^{-1}) was used for the ex situ encapsulation at 8 h, whereas the ZIF-8 obtained excluding caffeine from the synthesis solution (BET area = 1207 ± 10 m^2 g^{-1}) was used at 1.5−7 days.

Figure 2 compares the XRD patterns of commercial ZIF-8, CAF@ZIF-8_EX (8 h), CAF@ZIF-8_IN and pure caffeine. In

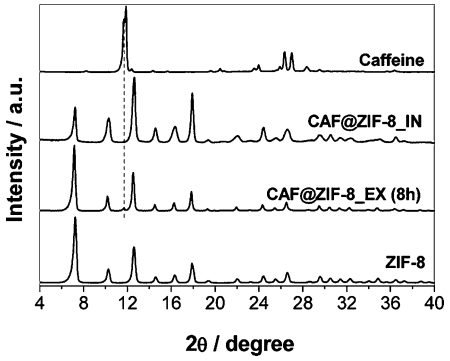

Figure 2. XRD patterns of CAF@ZIF-8_EX (8 h) and CAF@ZIF-8_IN; caffeine and commercial ZIF-8 patterns for comparison.

both CAF@ZIF-8 samples, the signals that agree with those of the commercial ZIF-8 used as a reference are evident. In addition, a peak at 11.7° denotes the presence of some free caffeine in CAF@ZIF-8_EX (8 h), while the large amount of caffeine dispersed at the molecular level in CAF@ZIF-8_IN provokes an important decrease in the intensity at 7.3°. Returning to Figure 1, 5 days appears to be the equilibrium encapsulation time; however, after 3 days, changes in the XRD patterns were noticeable (see Figure S3 in the Supporting Information). In consequence, for comparison purposes only CAF@ZIF-8_EX obtained after 8 h (CAF@ZIF-8_EX (8 h)) and 3 days (CAF@ZIF-8_EX (3d)) are considered from here.

Concerning thermal behavior, caffeine from CAF@ZIF-8_EX (8 h) left the material at about 150−240 °C, at the same temperature as that observed for pure caffeine (see Figure S1 in the Supporting Information). Therefore, no thermal stabilization was achieved at short contact times with the two-step encapsulation method. However, the release of caffeine from CAF@ZIF-8_IN and CAF@ZIF-8_EX (3d) started at about 425 °C so that a thermal enhancement of approximately 200 °C was achieved (see also the derivatives in the inset of Figure S1 in the Supporting Information). Besides the caffeine weight loss attributed to this sample, above 100 °C, the methanol solvent is lost and the 2-methylimidazole is probably protonated from the surfaces of the ZIF-8 crystals,[29] in addition to free caffeine not properly encapsulated. The stability of the materials prepared was also studied by thermal treatment during 10 min at 150, 260, 300, and 400 °C, and no apparent degradation was observed for CAF@ZIF-8_IN (Figure S4) as compared to CAF@ZIF-8_EX (8 h) (see Figure S5 in the Supporting Information) and ZIF-8 (see Figure S6 in the Supporting Information). This agrees with the previously high thermal stability reported for ZIF-8.[22,25,30] An additional proof of the thermal stability is provided by the XRD patterns obtained from ZIF-8 and CAF@ZIF-8_IN exposed to 450 °C (a temperature at which the release of caffeine has started, Figure S1in the Supporting Information) for 30 min. As shown in Figure S7 in the Supporting Information, the remaining caffeine exerts a certain stabilizing effect and CAF@ZIF-8 seems to be less affected than ZIF-8, which presents a few new intensities.

Both CAF@ZIF-8_IN and ZIF-8 crystals obtained in the conditions of CAF@ZIF-8_IN but without caffeine have homogeneous particle sizes of about 200−300 nm, as shown in Figure S9 in the Supporting Information. The synthesis of ZIF-8 either in water[30] or methanol[29] has already been reported; however, the combined use of water and methanol as solvents not only allowed a suitable crystal size for producing composites[26,31] minimizing agglomeration (contrary to what occurs with commercial ZIF-8, see Figure S8 in the Supporting Information) but also a high degree of caffeine loading.

Caffeine delivery was studied by UV absorption on CAF@ZIF-8_EX, obtained after 8 h and 3 days, and CAF@ZIF-8_IN materials. As depicted in Figure 3, the most important result is

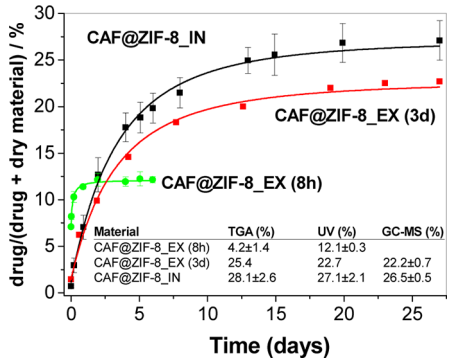

Figure 3. Caffeine delivery as determined by UV absorption from CAF@ZIF-8_EX (8 h), CAF@ZIF-8_EX (3d) and CAF@ZIF-8_IN in water. The inset table shows total amounts of encapsulated caffeine as obtained by TGA and UV.

that caffeine was released from CAF@ZIF-8_EX (8 h) after only 3 days, whereas CAF@ZIF-8_IN and CAF@ZIF-8_EX (3d) were continuously releasing the drug for 27 days. Such long times (20 days) have been reported for ibuprofen@MIL-53 released in a simulated body fluid.[32] The quantitative determination of caffeine in the solution allowed the verification of caffeine loading values (see inset table in Figure 3): 27.1 ± 2.1 wt % (28.1 ± 2.6 wt % by TGA), 22.7 wt % (25.4 wt % by TGA), and 12.1 ± 0.3 wt % (4.2 ± 1.4 wt % by TGA) for in situ and ex situ 3 days and 8 h encapsulations, respectively, in good agreement with the TGA values in brackets (and hence with weight loss assignments). The discrepancy for UV and TGA values in the case of CAF@ZIF-8_EX (8 h) accounts for the presence of free caffeine, in agreement with the XRD analysis (the peak observed at 11.7° in Figure 2) and not considered from TGA since, as mentioned above, encapsulation was considered only above 325 °C. The errors in Figure 3 were generated from the repetition of the delivery experiments with different batches of CAF@ZIF-8_IN (3) and CAF@ZIF-8_EX (8 h) (2), evidence of good reproducibility. Finally, the possible decomposition of CAF@ZIF-8_IN during the release process was also studied by XRD, finding that the ZIF-8 structure remains unchanged (see Figure S9 in the Supporting Information) at least for the first 8 days (78% released, Figure 3), whereas a few new peaks appeared after 15 days (94% released, Figure 3).

The continuous lines in Figure 3 were obtained applying eq 1

$$X_A = 1 - [k_1(n-1)t + k_2]^{1/(1-n)} \quad (1)$$

where X_A is the amount released (g of caffeine per g of caffeine + g of dry solid), t the time (days), and k_1 (day^{-1}), k_2, and n

constants. The regression factors (R^2) were above 0.99, whereas k_1, k_2, and n values are in Table 1. As expected, constants are similar for CAF@ZIF-8_IN and CAF@ZIF-8_EX (3d) and larger for CAF@ZIF-8_EX (8 h).

Table 1. Parameter Values According to Eq 1

sample	k_1 (day^{-1})	k_2 (day^{-1})	n	R^2
CAF@ZIF-8_EX (8h)	18 ± 7	2.3 ± 0.5	1.9 ± 0.2	0.994
CAF@ZIF-8_EX (3d)	0.31 ± 0.05	1.0 ± 0.0	1.4 ± 0.2	0.993
CAF@ZIF-8_IN	0.30 ± 0.03	1.0 ± 0.0	1.4 ± 0.1	0.996

Additional evidence of caffeine encapsulation is the decrease in the BET specific surface area of CAF@ZIF-8_IN (338 ± 21 m^2 g^{-1}) and the analysis by GC-MS of CAF@ZIF-8_IN and CAF@ZIF-8_EX (3d) solutions recovered at the end of the corresponding release experiments, which revealed encapsulation values (average of three analyses) of 26.5 ± 0.5 wt % and 22.2 ± 0.7 wt %, respectively, in good agreement with previous TGA and UV observations. After release for 8 days, CAF@ZIF-8_IN shows a BET area of 703 ± 15 m^2 g^{-1}, in agreement with the presence of some caffeine and some structural damage already commented.

^{13}C CP MAS NMR spectra where achieved for the pure caffeine, ZIF-8, and CAF@ZIF-8_EX (8 h) and CAF@ZIF-8_IN samples. Peaks corresponding to methyl groups of caffeine (Figure 4) are clearly seen only in sample CAF@ZIF-8_IN (28.6−33.8 ppm) with a notable chemical shift as compared to pure caffeine (30.0−36.8 ppm). The lower shift values of the methyl groups in encapsulated caffeine are due to shielding by the ZIF-8 structure. The rest of the caffeine peaks, even if hardly seen in CAF@ZIF-8_IN, suggest no π-type complexation with C=C (107.5 ppm) and do not allow C=N (144.0 ppm) and C=O (152.7 and 155.7 ppm) contributions to caffeine-ZIF-8 interaction to be discerned. The latter is explained by the ZIF-8 shifts. Although the carbon atom between the two nitrogen atoms of the imidazole-ring in ZIF-8 does not shift its signal (152.6 ppm), the methyl groups undergo a noticeable change from 15.2 ppm in pure ZIF-8 to 16.1 ppm in CAF@ZIF-8_IN. This change, together with that of the caffeine methyl groups, suggests van der Waals forces between the methyl groups in host and guest. Furthermore, important differences can be inferred from Figure 4 between ZIF-8 (125.6 ppm) and CAF@ZIF-8_EX (8 h) (125.6 ppm) and CAF@ZIF-8_IN (127.5 ppm) due to the hydrogen atoms of the double carbon bond (CH group[34]) of 2-methylimidazole. This points to hydrogen bond interaction of this CH with C=O in caffeine. A similar interaction (CH···O hydrogen bonds) has been described in caffeine crystals[35] in the liquid phase dimerization of cyclohexenone[36] and in other different examples,[37] and was confirmed here by FTIR analysis. In fact, the two main bands belonging to carbonyl (C=O) vibrations[38] at 1660 and 1705 cm^{-1} were monitored by FTIR. In both in situ and ex situ samples these bands are present in addition to the typical ZIF-8 bands.[22] Figure S10 in the Supporting Information shows a shift in ν(C=O) of encapsulated samples from about 1658 and 1702 cm^{-1} for pure caffeine to 1670 and 1712 cm^{-1} in CAF@ZIF-8_IN. The same effect, although slighter, is shown for CAF@ZIF-8_EX (8 h) (1667 and 1709 cm^{-1}). These shifts confirm the interactions between caffeine molecules and ZIF-8 CH groups deduced from NMR. Finally, the vibration at 1090 cm^{-1}, linked to C−N symmetric stretching,[39] was higher in CAF@ZIF-8_EX (8 h) than ZIF-8, and even higher in CAF@ZIF-8_IN. This may be related to the methyl−methyl interactions. Therefore, the methyl groups (van der Waals forces) and the hydrogen atoms (hydrogen bonds) from the double carbon bond of 2-methylimidazole in ZIF-8 constitute the preferred adsorption sites for caffeine encapsulated molecules.

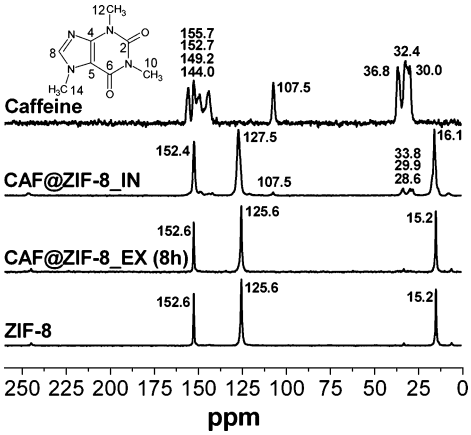

Figure 4. ^{13}C CP MAS NMR spectra of CAF@ZIF-8_EX (8 h) and CAF@ZIF-8_IN; caffeine and commercial ZIF-8 spectra for comparison. The observed chemical shifts (in ppm) for caffeine correspond to 30.0 (C10), 32.4 (C12), 36.8 (C14), 107.5 (C5), 144.0 (C8), 149.2 (C4), 152.7 (C2), and 155.7 (C6).[33].

If FTIR has confirmed interaction via carbonyl groups, N 1s XPS spectra recorded for the different samples in the study (Figure 5) will reinforce the hypothesis of methyl−methyl interaction. Two different nitrogen atoms are found in caffeine: three N−CH_3 (399.7 eV) and one N=C (398.0 eV), in agreement with the peak area ratio of three found in the pure caffeine spectrum. ZIF-8 exhibits a symmetric peak (399.1 eV) indicating that there is only one form of nitrogen. In both CAF@ZIF-8 samples, a new small band appears which means that there is a displacement of the main band (N−CH_3) in caffeine to 400.3 eV (ex situ) and 400.6 eV (in situ). This higher binding energy of N 1s orbital is because its charge is delocalized through the van der Waals interaction with methyl groups in ZIF-8 and the core attracts the electrons more strongly.

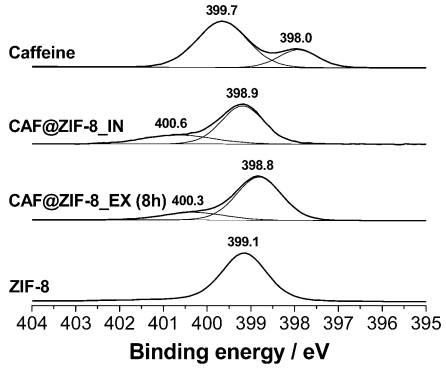

Figure 5. N 1s XPS spectra of CAF@ZIF-8_EX (8 h) and CAF@ZIF-8_IN; caffeine and commercial ZIF-8 spectra for comparison.

To gain insight into the encapsulation of caffeine in ZIF-8, powder XRD of CAF@ZIF-8_IN was analyzed by means of Materials Studio software. With the cubic $I\bar{4}3m$ space group

dx.doi.org/10.1021/am301365h | ACS Appl. Mater. Interfaces 2012, 4, 5016−5021

already reported for ZIF-8,[22] and using as initial estimation the cif file provided by Wong-Ng et al.,[40] a Rwp parameter of 6.55% was calculated for the successful refinement (Figure 6a). A cif

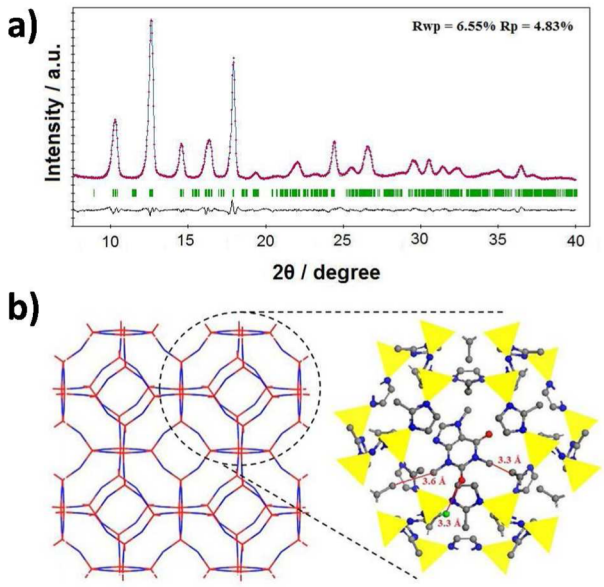

Figure 6. (a) Refinement of CAF@ZIF-8_IN; (b) ZIF-8 with the sod network along direction [100] (left) and detail of caffeine interactions with the MOF along direction [111] (right); blue, carbon; gray, nitrogen; red, oxygen; green, hydrogen; yellow tetrahedra, ZnO_4.

file corresponding to CAF@ZIF-8_IN is available as Supporting Information. Table S1 in the Supporting Information shows the parameters corresponding to the resolution of CAF@ZIF-8_IN and ZIF-8 obtained in the same conditions but without caffeine in the synthesis solution. In the case of CAF@ZIF-8_IN, the cell parameters obtained were $a = b = c = 17.150$ Å and $\alpha = \beta = \gamma = 90°$, which correspond with a cell volume of 5044 Å^3. These values are in agreement with those obtained by Park et al.[22] (a = 16.99 Å, V = 4905 Å^3) and with those obtained with the ZIF-8 prepared here (a = 17.084 Å, V = 4986 Å^3) and suggest some expansion of the structure to accommodate five molecules of caffeine per unit cell or cavity. This gives rise to the cell formula $Zn_{12}(MeIM)_{24}(CAF)_5$, where MeIM and CAF correspond to 2-methylimidazole and caffeine, respectively, and to a theoretical encapsulation of 28.1 wt %, in good agreement with the above-mentioned TGA and UV values. In addition, from the formula proposed (excluding Zn), C, H, N and O theoretical atomic compositions of 52.1, 6.4, 35.6, and 6.0%, respectively, can be calculated. They are in good agreement with those experimentally determined as 52.6, 5.7, 34.3, and 7.4%.

The best caffeine position obtained from the refinement has the methyl groups in the six-membered ring near the methyl groups of the organic linker in the ZIF-8 structure interacting by van der Waals forces, and in between these two methyl groups a carbonyl group interacting via hydrogen bond with a CH group in ZIF-8 (Figure 6b). Figure 6b suggests no π-interactions between caffeine and the organic linker, 2-methylimidazole, in agreement with the previous characterization and with the fact that caffeine and sulfamethoxazole did not complex.[41] A final comment must be made to the effect that ZIF-8, with cavities of 11.6 Å connected through 3.4 Å limiting small apertures,[22] allows both the encapsulation (by the one-step methodology implemented here) and release of caffeine molecules (6.1 × 7.6 Å). This is due to the flexibility that the organic linker induces in the MOF structure. In fact, the so-called gate-opening effect has been described before in ZIF-7[42] and ZIF-8[43] to explain adsorption−desorption of guest species with sizes larger than that of the corresponding MOF window.

CONCLUSIONS

We have succeeded in the in situ one-step encapsulation, at 25 °C for 2 h, of caffeine in ZIF-8 by demonstrating high guest loading (ca. 28 wt %) and controlled release (during 27 days). These features are due to simultaneous van der Waals interactions between caffeine and ZIF-8 imidazole methyl groups, and CH···O hydrogen bonds between hydrogen atoms in ZIF-8 imidazole groups and C═O groups in caffeine molecules. Besides requiring the previous synthesis of ZIF-8, the conventional two-step encapsulation, an ex situ method, needs at least 3 days at 80 °C to reach a similar encapsulation yield (ca. 25 wt %). Moreover, longer encapsulation times can damage the crystallinity of the material.

ASSOCIATED CONTENT

Supporting Information

Caffeine and 2-methylimidazole UV−vis spectra in water, TGA curves, XRD patterns of CAF@ZIF-8 powders at different encapsulation and release conditions and temperatures, SEM images, FTIR spectra, and resolution parameters for some of the materials obtained. This material is available free of charge via the Internet at http://pubs.acs.org.

AUTHOR INFORMATION

Corresponding Author

*E-mail: coronas@unizar.es.

Notes

The authors declare no competing financial interest.

ACKNOWLEDGMENTS

Financial support from the Spanish Ministry of Economy and Competitiveness (MAT2010-15870, IPT-2011-0878-420000) and the Aragón Government and ESF is gratefully acknowledged.

REFERENCES

(1) Ferey, G. *Chem. Soc. Rev.* **2008**, *37* (1), 191−214.
(2) Chae, H. K.; Siberio-Perez, D. Y.; Kim, J.; Go, Y.; Eddaoudi, M.; Matzger, A. J.; O'Keeffe, M.; Yaghi, O. M. *Nature* **2004**, *427* (6974), 523−527.
(3) Eddaoudi, M.; Kim, J.; Rosi, N.; Vodak, D.; Wachter, J.; O'Keeffe, M.; Yaghi, O. M. *Science* **2002**, *295* (5554), 469−472.
(4) Rose, M.; Bohringer, B.; Jolly, M.; Fischer, R.; Kaskel, S. *Adv. Eng. Mater.* **2011**, *13* (4), 356−360.
(5) Deng, H. X.; Doonan, C. J.; Furukawa, H.; Ferreira, R. B.; Towne, J.; Knobler, C. B.; Wang, B.; Yaghi, O. M. *Science* **2010**, *327* (5967), 846−850.
(6) An, J. Y.; Geib, S. J.; Rosi, N. L. *J. Am. Chem. Soc.* **2009**, *131* (24), 8376−8377.
(7) Zornoza, B.; Martinez-Joaristi, A.; Serra-Crespo, P.; Tellez, C.; Coronas, J.; Gascon, J.; Kapteijn, F. *Chem. Commun.* **2011**, *47* (33), 9522−9524.
(8) Lee, J.; Farha, O. K.; Roberts, J.; Scheidt, K. A.; Nguyen, S. T.; Hupp, J. T. *Chem. Soc. Rev.* **2009**, *38* (5), 1450−1459.
(9) Yang, Q. Y.; Zhong, C. L. *J. Phys. Chem. B* **2006**, *110* (36), 17776−17783.

(10) Horcajada, P.; Serre, C.; Vallet-Regi, M.; Sebban, M.; Taulelle, F.; Ferey, G. *Angew. Chem., Int. Ed.* **2006**, *45* (36), 5974−5978.
(11) Rieter, W. J.; Taylor, K. M. L.; An, H. Y.; Lin, W. L.; Lin, W. B. *J. Am. Chem. Soc.* **2006**, *128* (28), 9024−9025.
(12) Juan-Alcaniz, J.; Ramos-Fernandez, E. V.; Lafont, U.; Gascon, J.; Kapteijn, F. *J. Catal.* **2010**, *269* (1), 229−241.
(13) An, J. Y.; Shade, C. M.; Chengelis-Czegan, D. A.; Petoud, S.; Rosi, N. L. *J. Am. Chem. Soc.* **2011**, *133* (5), 1220−1223.
(14) (a) Sun, C. Y.; Liu, S. X.; Liang, D. D.; Shao, K. Z.; Ren, Y. H.; Su, Z. M. *J. Am. Chem. Soc.* **2009**, *131* (5), 1883−1888. (b) Bajpe, S. R.; Breynaert, E.; Mustafa, D.; Jobbagy, M.; Maes, A.; Martens, J. A.; Kirschhock, C. E. A. *J. Mater. Chem.* **2011**, *21* (26), 9768−9771.
(15) Juan-Alcaniz, J.; Goesten, M.; Martinez-Joaristi, A.; Stavitski, E.; Petukhov, A. V.; Gascon, J.; Kapteijn, F. *Chem. Commun.* **2011**, *47* (30), 8578−8580.
(16) Cai, Y.; Gaffney, S. H.; Lilley, T. H.; Magnolato, D.; Martin, R.; Spencer, C. M.; Haslam, E. *J. Chem. Soc., Perkin Trans. 2* **1990**, No. 12, 2197−2209.
(17) Touitou, E.; Junginger, H. E.; Weiner, N. D.; Nagai, T.; Mezei, M. *J. Pharm. Sci.* **1994**, *83* (9), 1189−1203.
(18) Rosenberg, R. T.; Siegel, S. J.; Dan, N. *J. Appl. Polym. Sci.* **2008**, *107* (5), 3149−3156.
(19) Katsikogianni, G.; Avgoustakis, K. *J. Nanosci. Nanotechnol.* **2006**, *6* (9−10), 3080−3086.
(20) Gunasekaran, S.; Ko, S.; Xiao, L. *J. Food Eng.* **2007**, *83* (1), 31−40.
(21) Wei, H. S.; Tsai, Y. L.; Wu, J. Y.; Chen, H. *J. Chromatogr., B: Anal. Technol. Biomed. Life Sci.* **2006**, *836* (1−2), 57−62.
(22) Park, K. S.; Ni, Z.; Cote, A. P.; Choi, J. Y.; Huang, R. D.; Uribe-Romo, F. J.; Chae, H. K.; O'Keeffe, M.; Yaghi, O. M. *Proc. Natl. Acad. Sci. U.S.A.* **2006**, *103* (27), 10186−10191.
(23) Gaudin, C.; Cunha, D.; Ivanoff, E.; Horcajada, P.; Chevé, G.; Yasri, A.; Loget, O.; Serre, C.; Maurin, G. *Microporous Mesoporous Mater.* **2012**, *157*, 124−130.
(24) Horcajada, P.; Chalati, T.; Serre, C.; Gillet, B.; Sebrie, C.; Baati, T.; Eubank, J. F.; Heurtaux, D.; Clayette, P.; Kreuz, C.; Chang, J. S.; Hwang, Y. K.; Marsaud, V.; Bories, P. N.; Cynober, L.; Gil, S.; Ferey, G.; Couvreur, P.; Gref, R. *Nat. Mater.* **2010**, *9* (2), 172−178.
(25) Low, J. J.; Benin, A. I.; Jakubczak, P.; Abrahamian, J. F.; Faheem, S. A.; Willis, R. R. *J. Am. Chem. Soc.* **2009**, *131* (43), 15834−15842.
(26) (a) Perez, E.; Martin, L.; Rubio, C.; Urieta, J. S.; Piera, E.; Caballero, M. A.; Tellez, C.; Coronas, J. *Ind. Eng. Chem. Res.* **2010**, *49* (18), 8495−8500. (b) Caballero, M. A.; Zagalaz, P.; Segura, S.; Piera, E.; Perez, E.; Tellez, C.; Coronas, J.; Santamaria, J. U.S. Patent US 2008/0128941 A1, 2008.
(27) Rietveld, H. M. *J. Appl. Crystallogr.* **1969**, *2*, 65−71.
(28) Pawley, G. S. *J. Appl. Crystallogr.* **1981**, *14*, 357−361.
(29) Cravillon, J.; Munzer, S.; Lohmeier, S. J.; Feldhoff, A.; Huber, K.; Wiebcke, M. *Chem. Mater.* **2009**, *21* (8), 1410−1412.
(30) Pan, Y.; Liu, Y.; Zeng, G.; Zhao, L.; Lai, Z. *Chem. Commun.* **2011**, *47* (7), 2071−2073.
(31) Zornoza, B.; Seoane, B.; Zamaro, J. M.; Téllez, C.; Coronas, J. *ChemPhysChem* **2011**, *12* (15), 2781−2785.
(32) Horcajada, P.; Serre, C.; Maurin, G.; Ramsahye, N. A.; Balas, F.; Vallet-Regi, M.; Sebban, M.; Taulelle, F.; Ferey, G. *J. Am. Chem. Soc.* **2008**, *130* (21), 6774−6780.
(33) Enright, G. D.; Terskikh, V. V.; Brouwer, D. H.; Ripmeester, J. A. *Cryst. Growth Des.* **2007**, *7* (8), 1406−1410.
(34) Chmelik, C.; Freude, D.; Bux, H.; Haase, J. *Microporous Mesoporous Mater.* **2012**, *147* (1), 135−141.
(35) de Matas, M.; Edwards, H. G. M.; Lawson, E. E.; Shields, L.; York, P. *J. Mol. Struct.* **1998**, *440* (1−3), 97−104.
(36) Nolasco, M. M.; Ribeiro-Claro, P. J. A. *ChemPhysChem* **2005**, *6* (3), 496−502.
(37) (a) Wendler, K.; Thar, J.; Zahn, S.; Kirchner, B. *J. Phys. Chem. A* **2010**, *114* (35), 9529−9536. (b) Sonoda, Y.; Goto, M.; Ikeda, T.; Shimoi, Y.; Hayashi, S.; Yamawaki, H.; Kanesato, M. *J. Mol. Struct.* **2011**, *1006* (1−3), 366−374.
(38) Paradkar, M. M.; Irudayaraj, J. *J. Food Sci.* **2002**, *67* (7), 2507−2511.
(39) Gunasekaran, S.; Sankari, G.; Ponnusamy, S. *Spectrochim. Acta Part A* **2005**, *61* (1−2), 117−127.
(40) Wong-Ng, W.; Kaduk, J. A.; Espinal, L.; Suchomel, M. R.; Allen, A. J.; Wu, H. *Powder Diffr.* **2011**, *26* (3), 234−237.
(41) Kesimli, B.; Topacli, A.; Topacli, C. *J. Mol. Struct.* **2003**, *645* (2−3), 199−204.
(42) (a) Gücüyener, C.; van den Bergh, J.; Gascon, J.; Kapteijn, F. *J. Am. Chem. Soc.* **2010**, *132* (50), 17704−17706. (b) Aguado, S.; Bergeret, G.; Titus, M. P.; Moizan, V.; Nieto-Draghi, C.; Bats, N.; Farrusseng, D. *New J. Chem.* **2011**, *35* (3), 546−550.
(43) Moggach, S. A.; Bennett, T. D.; Cheetham, A. K. *Angew. Chem., Int. Ed.* **2009**, *48* (38), 7087−7089.